Electronic Supplementary Material (ESI) for Physical Chemistry Chemical Physics.

Electronic Supplementary Information for

"Interlayer Coupling in Two-Dimensional Titanium Carbide MXenes"

Tao Hu,[ab] Minmin Hu,[ac] Zhaojin Li,[ab] Hui Zhang,[ab] Chao Zhang,[a] Jingyang Wang[a] and Xiaohui Wang*[a]

[a]*Shenyang National Laboratory for Materials Science, Institute of Metal Research, Chinese Academy of Sciences, 72 Wenhua Road, Shenyang 110016, China*

[b]*University of Chinese Academy of Sciences, Beijing 100049, China*

[c]*School of Materials Science and Engineering, University of Science and Technology of China, Hefei 230026, China*

Content

■ Methods

Calculation details

Ultrasoft potentials[1] were utilized for the calculations. The Monkhorst–Pack scheme[2] with 9 × 9 × 1 k point meshes were used for the integration in the irreducible Brillouin zone so that the individual spacing was less than 0.05 $Å^{-1}$. In line with our previous work,[3] the energy cutoff in the calculations was set to 380 eV. The Broyden–Fletcher–Goldfarb–Shanno minimization scheme[4] was used to minimize the total energy and interatomic forces. The Fermi level was smeared by 0.1 eV. The convergence for energy was chosen as 1.0×10^{-9} eV/atom, and the structures were relaxed until the maximum force exerted on the atoms became less than 0.001 eV/Å.

Bench mark calculation of long-range interaction

As a prerequisite, we first tested the validity of DFT-D on the simulation of long-range interaction in two model layered materials like graphite (the graphite in this study is referred to as *AB* stacking graphite unless specified otherwise) and MoS_2. The calculated lattice parameters and binding energies agree well with the experimentally determined values, demonstrating that DFT-D is reliable in the simulation of long-range interaction in layered materials (Table S1 in the Supporting Information). The calculated binding energies with the two schemes of DFT and DFT-D are summarized in Fig. S2 in the Supporting Information. As shown in Fig. S2, the long-range interaction plays an indispensable role in the layered materials $Ti_{n+1}C_nT_2$ as well as in graphite and MoS_2. Neglecting the long-range interaction may cause inaccuracy or even mistakes. Therefore, in the investigation of interlayer coupling of MXenes in this work, long-range interaction was taken into consideration by using the DFT-D scheme.

Young's modulus calculation

The validity of the results of Young's modulus can be examined by calculating the Young's moduli of graphite and MoS_2 with the same scheme. The calculated results are close to experimental results (graphite, 36 GPa, which is measured to be 34 GPa;

MoS_2, 26 GPa, the experimental result is 19 GPa). The optimized structural configuration and total energy under each strain pattern are obtained by full relaxation with constraint of the strain. To ensure that the material is under uniaxial tension, lattice vectors in the transverse direction and internal atomic positions were fully relaxed at each pre-set strain.

■ Tables

Table S1. Bench mark calculation: Calculated and experimental lattice constants and stacking energies of graphite and MoS_2 with DFT and DFT-D

Graphite				
method	DFT	DFT-D		Ref.
functional	PBE	Grimme	OBS	
***a* (Å)**	2.47	2.46	2.46	2.46[a]
***c* (Å)**	11.74	6.43	6.75	6.70[a]
***d* (Å)**	5.87	3.22	3.33	3.35[a]
E_b (J/m^2)	−0.01	0.26	0.52	0.36[b], 0.37[c], 0.32[d], 0.29[e], 0.58[f]
MoS_2				
method	DFT	DFT-D		Ref.
functional	PBE	Grimme	OBS	
***a* (Å)**	3.18	3.19	3.18	3.16[g]
***c* (Å)**	15.40	12.46	12.74	12.30[g]
***d* (Å)**	4.59	3.13	3.25	3.08[g]
E_b (J/m^2)	0.01	0.29	0.37	0.22[h], 0.33[i], 0.52[j], 0.56[k]

[a]Ref. 5 (exp.), [b]Ref. 6 (exp.), [c]Ref. 7 (exp.), [d]Ref. 8 (cal.), [e]Ref. 9 (cal.), [f]Ref. 10 (cal.), [g]Ref. 11 (exp.), [h]Ref. 12(exp.), [i]Ref. 9 (cal.), [j]Ref. 13 (cal.), [k]Ref. 14 (cal.)

Table S2. Calculated lattice constants of stacked bare Ti_3C_2 and $Ti_3C_2T_2$ (T = OH, O, and F) with three schemes of DFT-D

formula	a (Å)	c (Å)
SH-$Ti_3C_2(OH)_2$	3.05[a], 3.07[b], 2.98[c]	21.88[a], 24.03[b], 21.67[c]
Bernal-$Ti_3C_2(OH)_2$	3.06[a], 3.09[b], 3.00[c]	19.28[a], 19.67[b], 18.70[c]
SH-$Ti_3C_2O_2$	3.02[a], 3.03[b], 2.97[c]	19.43[a], 20.04[b], 18.79[c]
Bernal- $Ti_3C_2O_2$	3.02[a], 3.04[b], 2.97[c]	18.59[a], 18.93[b], 17.85[c]
SH-$Ti_3C_2F_2$	3.05[a], 3.07[b], 2.99[c]	19.72[a], 20.24[b], 19.05[c]
Bernal-$Ti_3C_2F_2$	3.05[a], 3.07[b], 3.00[c]	18.70[a], 19.02[b], 17.84[c]
SH-Ti_3C_2	3.03[a], 3.06[b], 2.98[c]	14.88[a], 15.06[b], 14.54[c]
Bernal-Ti_3C_2	3.05[a], 3.08[b], 3.00[c]	14.44[a], 14.66[b], 14.14[c]

[a]GGA-PW91-OBS; [b]GGA-PBE-Grimme; [c]LDA-OBS-CAPZ

Table S3. Binding energies of two stacked models of bare Ti_2C and Ti_2CT_2 (T = OH, O, and F) along [0001][a]

formula	$E_{stacked}$ (eV)	$E_{monolayer}$ (eV)	a (Å)	E_b (J/m²)
Bernal-$Ti_2C(OH)_2$	–4277.12926	–4276.09380	3.04871	2.0583
Bernal-Ti_2CO_2	–4245.04306	–4244.48968	3.02486	1.1174
Bernal-Ti_2CF_2	–4696.54187	–4696.01418	3.04024	1.0548
Bernal-Ti_2C	–3366.44361	–3363.76173	3.00366	5.4921
SH-$Ti_2C(OH)_2$	–8553.30416	–4276.09380	3.03127	1.1225
SH-Ti_2CO_2	–8489.98124	–4244.48968	3.0117	1.0204
SH-Ti_2CF_2	–9392.90569	–4696.01418	3.03282	0.8811
SH-Ti_2C	–6732.58044	–3363.76173	2.99486	5.2085
graphite	–621.81029	–310.73408	2.45388	0.5249
MoS_2	–4994.97833	–2497.28903	3.17673	0.3664

[a] Calculated with GGA-PW91-OBS

Table S4. Binding energies of two stacked models of bare Ti_3C_2 and $Ti_3C_2T_2$ (T = OH, O, and F) along [0001]

functional	formula	$E_{stacked}$ (eV)	$E_{monolayer}$ (eV)	a (Å)	E_b (J/m^2)
GGA-PW91-OBS	Bernal-$Ti_3C_2(OH)_2$	−12078.07017	−6037.92671	3.06204	2.1841
	Bernal-$Ti_3C_2O_2$	−12013.65137	−6006.15310	3.02113	1.3615
	Bernal-$Ti_3C_2F_2$	−12916.90820	−6457.84416	3.05759	1.2054
	Bernal-Ti_3C_2	−10257.05786	−5125.69117	3.05173	5.6297
	SH-$Ti_3C_2(OH)_2$	−12076.97690	−6037.92671	3.04904	1.1164
	SH-$Ti_3C_2O_2$	−12013.45801	−6006.15310	3.01649	1.1694
	SH-$Ti_3C_2F_2$	−12916.71214	−6457.84416	3.05057	1.0163
	SH-Ti_3C_2	−10256.64232	−5125.69117	3.03538	5.2739
	graphite	−621.8102899	−310.73408	2.45388	0.5249
	MoS_2	−4994.978328	−2497.28903	3.17673	0.3664
GGA-PBE-Grimme	Bernal-$Ti_3C_2(OH)_2$	−12067.90244	−6033.66962	3.08909	0.5452
	Bernal-$Ti_3C_2O_2$	−12004.67128	−6002.17839	3.03792	0.3180
	Bernal-$Ti_3C_2F_2$	−12907.44947	−6453.57820	3.07198	0.2869
	Bernal-Ti_3C_2	−10249.70814	−5122.71214	3.08142	4.1678
	SH-$Ti_3C_2(OH)_2$	−12067.58456	−6033.66962	3.07113	0.2402
	SH-$Ti_3C_2O_2$	−12004.55624	−6002.17839	3.03502	0.2000
	SH-$Ti_3C_2F_2$	−12907.34595	−6453.57820	3.06952	0.1858
	SH-Ti_3C_2	−10249.18490	−5122.71214	3.06461	3.6990
	graphite	−620.72495	−310.27721	2.46057	0.2602
	MoS_2	−4992.564934	−2496.12446	3.18862	0.2871
LDA-CAPZ-OBS	Bernal-$Ti_3C_2(OH)_2$	−12070.33969	−6033.71385	3.00282	2.9833
	Bernal-$Ti_3C_2O_2$	−12006.38621	−6002.30131	2.97349	1.8635
	Bernal-$Ti_3C_2F_2$	−12903.76034	−6451.05582	2.99985	1.6924
	Bernal-Ti_3C_2	−10251.89207	−5122.8382	2.99998	6.3801
	SH-$Ti_3C_2(OH)_2$	−12068.87452	−6033.71385	2.98098	1.5040
	SH-$Ti_3C_2O_2$	−12006.05460	−6002.30131	2.96586	1.5249
	SH-$Ti_3C_2F_2$	−12903.38552	−6451.05582	2.99215	1.3144
	SH-Ti_3C_2	−10251.47788	−5122.83816	2.97776	6.0442
	graphite	−622.93556	−311.18187	2.43227	0.8929
	MoS_2	−4991.88344	−2495.51630	3.10253	0.8166

Table S5. Total energies and binding energies of two stacked models of half-half terminated $Ti_3C_2T_2$ (*T* = OH, O, and F) along [0001] with GGA-PW91-OBS. The most stable configurations are highlighted in bold

formula	$E_{stacked}$ (eV)	E_b (J/m^2)
Bernal-O(OH)	−12046.67853	2.6781
Bernal-F(OH)	−12497.60829	1.7994
Bernal-OF	**−12465.19749**	1.3588
SH-O(OH)	**−12047.23176**	3.3169
SH-F(OH)	**−12497.68819**	1.8772
SH-OF	−12465.00644	1.1684

Table S6. Total energies of Nb_2CT_2 (*T* = OH, O, and F) monolayer with *T* locate at different site. GGA-PBE was used and the spin was also taken into consideration. The most stable configurations are highlighted in bold

Nb_2C	O	F	OH
I	**−4135.9240**	**−4586.6292**	**−4166.7694**
II	−4135.3667	−4586.4071	−4166.7362

I, the hollow site of three C atoms; II, the hollow site of three Nb atoms.

Table S7. Binding energies of two stacked models of Ti_2CT_2, Nb_2CT_2 and Ti_2NT_2 (*T* = OH, O, and F) along [0001] with GGA-PW91-OBS. The most stable configuration of Ti_2NT_2 according to ref. 15 is used

formula	Ti_2CT_2	Nb_2CT_2	Ti_2NT_2
Bernal-OH	2.0583	1.7678	1.9018
Bernal-O	1.1174	1.1406	1.1997
Bernal-F	1.0548	0.9631	1.0291
SH-OH	1.1225	1.0977	1.1330
SH-O	1.0204	0.9169	1.0157
SH-F	0.8811	0.7134	0.9004

Figures

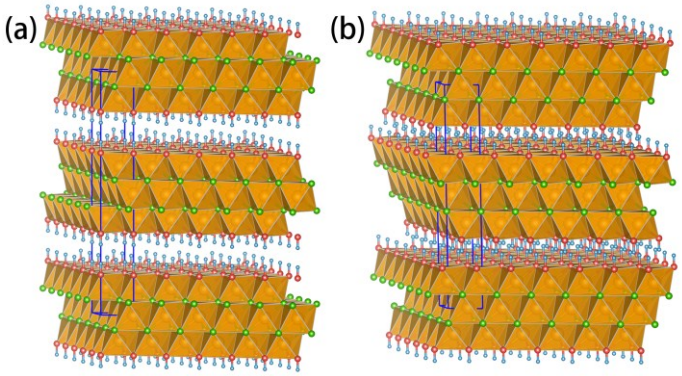

Fig. S1 Polyhedral models of two distinct $Ti_3C_2(OH)_2$ stacking types. (a) SH stacking, and (b) Bernal stacking. The terminations stabilize the layered structure by retaining Ti-centered Ti(C,*T*)$_6$ octahedra.

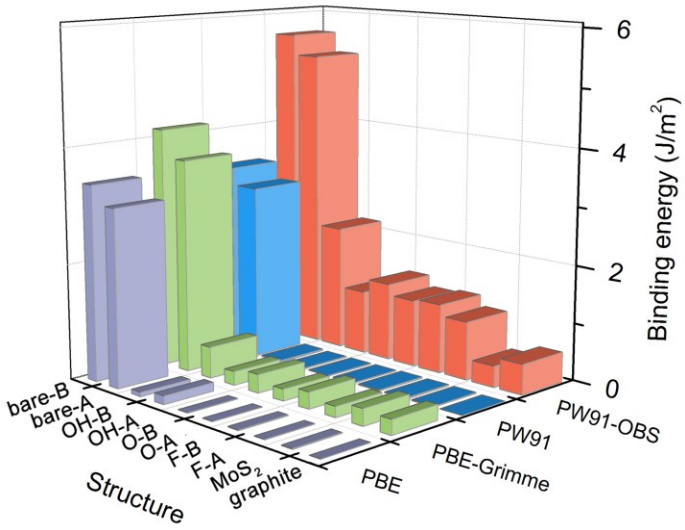

Fig. S2 Binding energies of stacked bare Ti_3C_2 and terminated $Ti_3C_2T_2$ (*T* = O, F, and OH), graphite and MoS_2 with DFT and DFT-D. A stands for SH stacking, and B is short for Bernal stacking. Note that the binding energies of graphite, MoS_2, and *T*-functionalized $Ti_3C_2T_2$ calculated with DFT approximate to zero compared with those calculated with DFT-D. The big difference in binding energy calculated with DFT and DFT-D indicates the long-range interaction plays an indispensable role in MXenes as well as graphite and MoS_2.

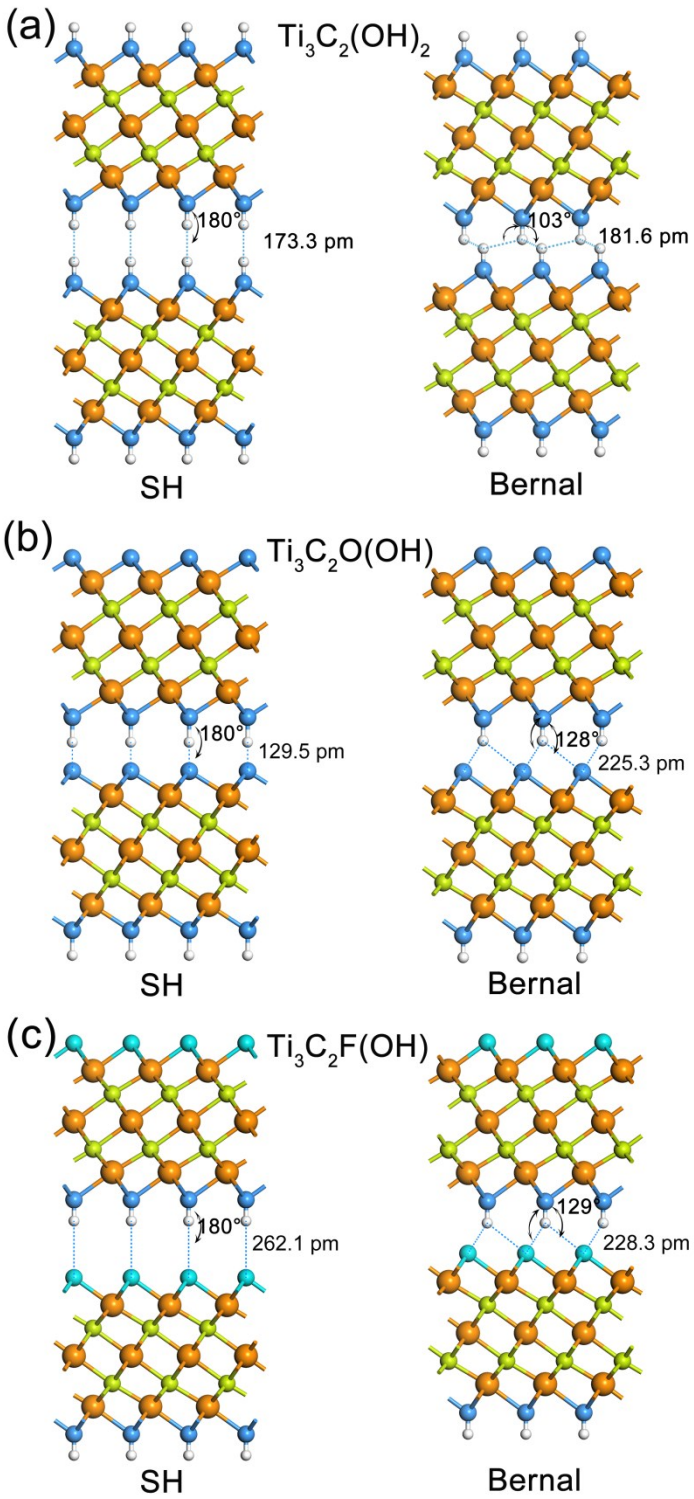

Fig. S3 Configuration of hydrogen bonds in stacked $Ti_3C_2T_2$. (a) SH and Bernal $Ti_3C_2(OH)_2$; (b) SH and Bernal $Ti_3C_2O(OH)$; (c) SH and Bernal $Ti_3C_2F(OH)$. Note that both the bond length and bond angle of stacked $Ti_3C_2(OH)_2$ are in the range of dihydrogen bond[16,17].

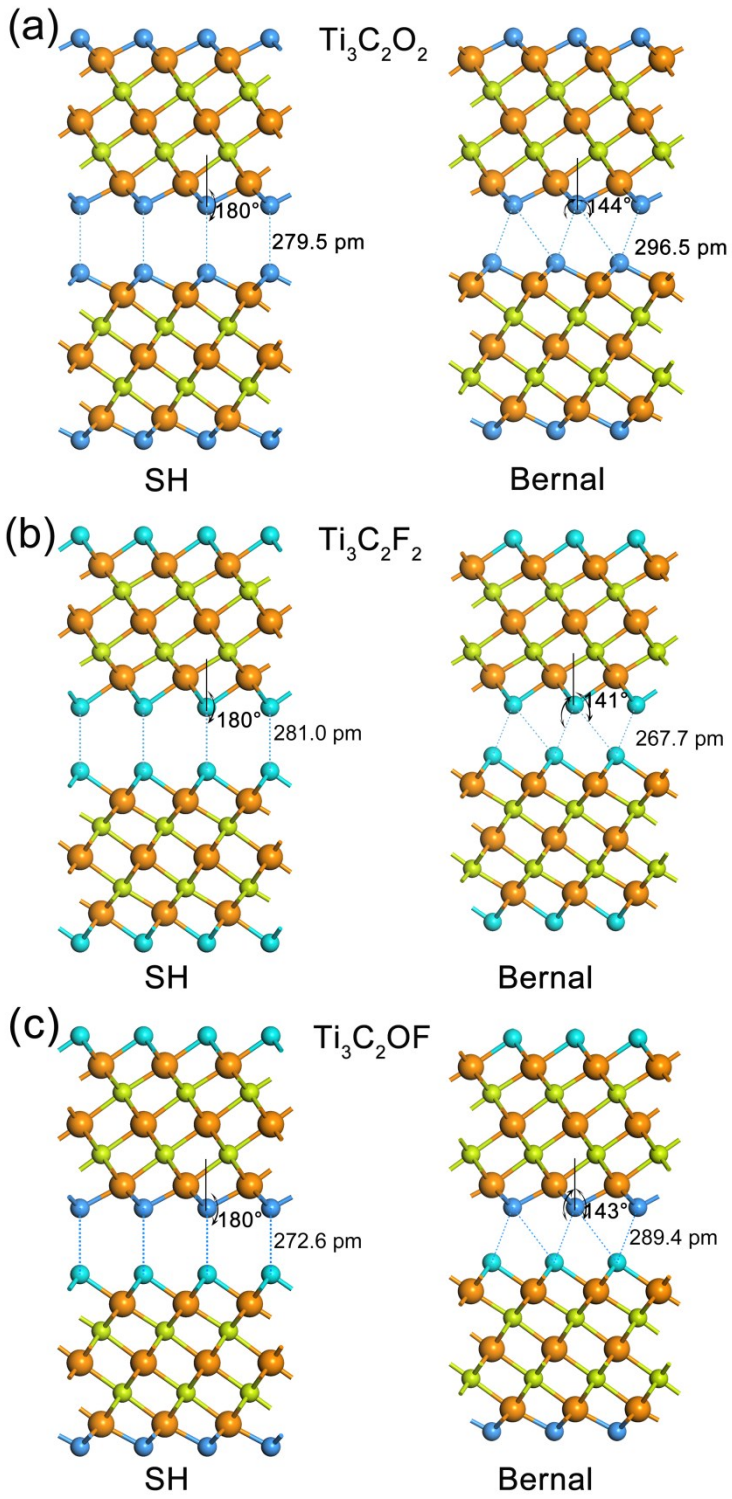

Fig. S4 Configuration of intermolecular bonds in stacked $Ti_3C_2T_2$. (a) SH and Bernal $Ti_3C_2O_2$; (b) SH and Bernal $Ti_3C_2F_2$; (c) SH and Bernal Ti_3C_2OF.

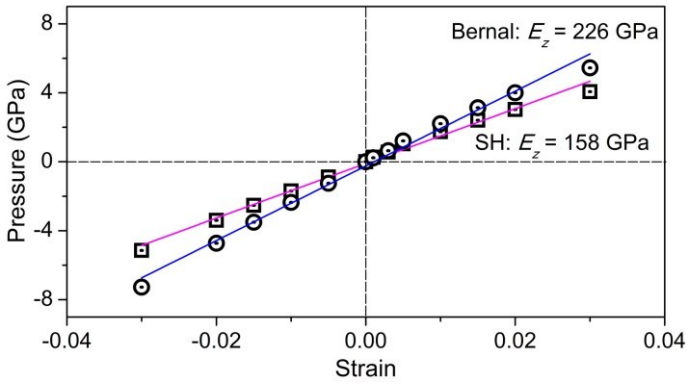

Fig. S5 Fitted lines for calculating the Young's modulus along [0001] in stacked $Ti_3C_2(OH)_2$. The fitted Young's moduli along [0001] are 158 and 226 GPa for SH and Bernal stacked $Ti_3C_2(OH)_2$, respectively. The structures are fully relaxed while retain the strain along z axis.

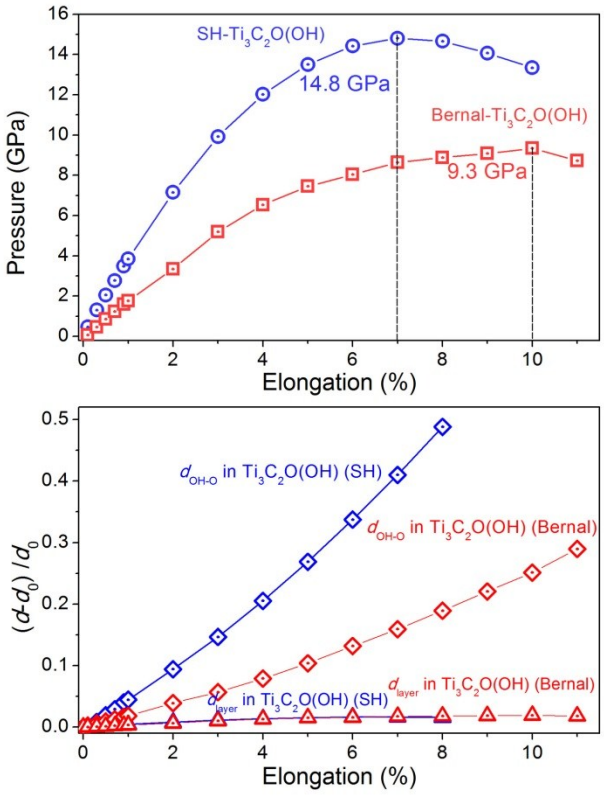

Fig. S6 Atomistic elongation simulation of stacked $Ti_3C_2O(OH)$ along [0001]. (a) Stress−elongation curves in a simulation of tension procedure along the *c* direction of two types of stacked $Ti_3C_2O(OH)$. (b) Interlayer distance and layer thickness in a simulation of tension procedure along the *c* direction.

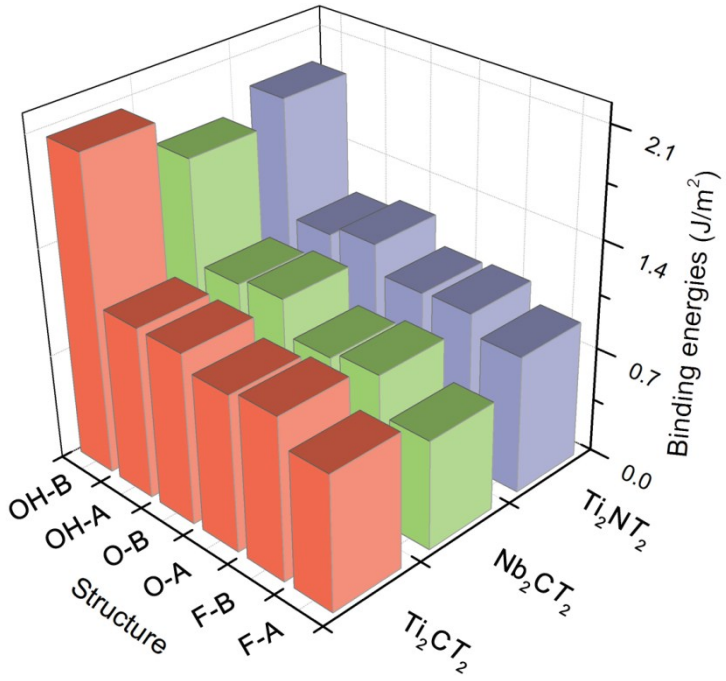

Fig. S7 Binding energies of two stacked models of Ti_2CT_2, Nb_2CT_2 and Ti_2NT_2 (T = OH, O, and F) along [0001]. The trends are similar. The primary mode that holds the MXenes stacked are hydrogen bonds and intermolecular interactions, which are much stronger than van der Waals coupling in graphite and MoS_2.

REFERENCES

1 G. Kresse and J. Furthmuller, *Phys. Rev. B*, 1996, **54**, 11169–11186.

2 M. Methfessel and A. Paxton, *Phys. Rev. B* 1989, **40**, 3616–3621.

3 T. Hu, H. Zhang, J. M. Wang, Z. J. Li, M. M. Hu, J. Tan, P. X. Hou, F. Li and X. H. Wang, *Sci. Rep.*, 2015, **5**, 16329.

4 T. H. Fischer and J. Almlof, *J. Phys. Chem.*, 1992, **96**, 9768–9774.

5 Y. Zhao and I. Spain, *Phys. Rev. B*, 1989, **40**, 993–997.

6 R. Zacharia, H. Ulbricht and T. Hertel, *Phys. Rev. B*, 2004, **69**, 155406.

7 W. Wang, S. Y. Dai, X. D. Li, J. R. Yang, D. J. Srolovitz and Q. S. Zheng, *Nat. Commun.*, 2015, **6**, 7853.

8 J. Dai and X. C. Zeng, *Angew. Chem., Int. Ed.*, 2015, **54**, 7572–7576.

9 T. Björkman, A. Gulans, A. V. Krasheninnikov and R. M. Nieminen, *Phys. Rev. Lett.*, 2012, **108**, 235502.

10 S. Lebègue, J. Harl, T. Gould, J. G. Ángyán, G. Kresse and J. F. Dobson, *Phys. Rev. Lett.*, 2010, **105**, 196401.

11 J. N. Coleman, M. Lotya, A. O'Neill, S. D. Bergin, P. J. King, U. Khan, K. Young, A. Gaucher, S. De, R. J. Smith, I. V. Shvets, S. K. Arora, G. Stanton, H. Kim, K. Lee, G. T. Kim, G. S. Duesberg, T. Hallam, J. J. Boland, J. J. Wang, J. F. Donegan, J. C. Grunlan, G. Moriarty, A. Shmeliov, R. J. Nicholls, J. M. Perkins, E. M. Grieveson, K. Theuwissen, D. W. McComb, P. D. Nellist and V. Nicolosi, *Science*, 2011, **331**, 568–571.

12 D. M. Tang, D. G. Kvashnin, S. Najmaei, Y. Bando, K. Kimoto, P. Koskinen, P. M. Ajayan, B. I. Yakobson, P. B. Sorokin, J. Lou and D. Golberg, *Nat. Commun.*, 2014, **5**, 3631.

13 K. Weiss and J. M. Phillips, *Phys. Rev. B*, 1976, **14**, 5392–5395.

14 J. D. Fuhr, J. O. Sofo and A. Saul, *Phys. Rev. B*, 1999, **60**, 8343–8347.

15 Y. Xie and P. R. C. Kent, *Phys. Rev. B*, 2013, **87**, 235441.

16 W. K. Li, G. D. Zhou and T. C. W. Mak, *Advanced Structural Inorganic Chemistry*. (Oxford university press, 2008).

17 V. I. Bakhmutov, *Dihydrogen Bonds*. (John Wiley & Sons, 2008).